Acta Cryst. (1975). A31, 846

The Structures of $Na_{0.98}K_{0.02}NbO_3$ and $Na_{0.90}K_{0.10}NbO_3$ (Phase *Q*) at Room Temperature by Neutron Powder Diffraction

BY M. AHTEE
Department of Physics, University of Helsinki, Helsinki, Finland
AND A. W. HEWAT
Institut Laue-Langevin, Grenoble, France

(*Received* 11 *June* 1975; *accepted* 16 *June* 1975)

The phase-*Q* structures of $Na_{0.98}K_{0.02}NbO_3$ and $Na_{0.90}K_{0.10}NbO_3$ have been determined at room temperature by the neutron powder profile refinement technique. Two different models were refined: orthorhombic, space group $P2_1ma$ (No. 26, in *cab* setting) and monoclinic, space group *Pm* (No. 6, in the second setting). The latter is more correct as it takes into account the splitting of the monoclinic a_p and c_p, but the structures can be described as very nearly orthorhombic. In the 2 mole % structure Nb atoms are all displaced by 0·18 (1) Å in the same direction towards the midpoint of the edge of the surrounding octahedron. The octahedra themselves appear to be regular and are tilted by 6·8 (1)° around a_p and c_p and by 7·8 (1)° around b_p. Na, K displacements [0·23 (4) Å] are almost parallel to those of Nb. For the 10 mole % structure Na, K and Nb displacements are the same but the tilts (5·2° and 7·3°) are somewhat smaller.

1. Introduction

$NaNbO_3$ and $KNbO_3$ form a continuous solid solution. The perovskite system $Na_{1-x}K_xNbO_3$ has been extensively studied because it shows a number of ferroelectric phases with high spontaneous polarization. Na, K niobate ceramics are also attractive for their piezoelectric applications. Very little, however, is known about the structures of the intermediate phases and their relationship to the observed macroscopic properties. To get a detailed picture of what occurs during structural changes, the magnitudes and directions of the atomic displacements are required.

Single-crystal diffraction experiments are difficult with ferroelectric materials of the perovskite type because of the difficulty of getting good untwinned single crystals. On the other hand, it is a simple matter to obtain a diffraction pattern from a powder sample. Here the problem is the analysis of the complicated patterns. Recently, Hewat (1973, 1974*a*) has applied profile analysis of the neutron powder diffraction pattern (Rietveld, 1969) to the structure determination of $KNbO_3$ and the room-temperature phase *P* of pure $NaNbO_3$. His results compare favourably with those obtained from single-crystal X-ray measurements.

The present study is a continuation of the work by Ahtee & Glazer (1974, 1975). The aim is to determine the structural details of the $Na_{1-x}K_xNbO_3$ solid solutions in the region $x=0{\cdot}6$–10 mole % at room temperature. We call this phase *Q* using the notation adopted earlier by Megaw for the induced ferroelectric phase of pure $NaNbO_3$. The relations between the structures of phase *Q* and the system $Na_{0.975}K_{0.025}NbO_3$ has been discussed by Wells & Megaw (1961), Wood, Miller & Remeika (1962) and Lefkowitz, Łukaszewicz & Megaw (1966).

According to dielectric measurements (Cross, 1958) the antiferroelectric phase *P* of pure $NaNbO_3$ extends up to the composition 0·6 mole % $KNbO_3$. Above that the mixed crystals give ferroelectric hysteresis loops. However, in the region 0·6–1·6 mole % the ferroelectric and antiferroelectric phases coexist. Therefore we have chosen the 2 mole % solid solution to represent phase *Q*. We also measured the 10 mole % sample to see the changes of the parameters over the whole region.

The structure of $Na_{0.975}K_{0.025}NbO_3$ has been determined (Wells & Megaw, 1961) by single-crystal X-ray diffraction. The refinement was incomplete and only a short description of the structure was given. Later, in connexion with the structure determination of phase *P* of $NaNbO_3$, Sakowski-Cowley, Łukaszewicz & Megaw (1969) have predicted the main features of the structure. They have also explained why the direction of the Nb displacements reverses with the tilts. But, as they say, the details are subject to confirmation.

2. Specimen preparation and diffraction measurements

Samples were prepared following closely the mixing and calcining procedure employed by Tennery & Hang (1968). The raw materials were Na_2CO_3 and K_2CO_3 (reagent grade products of E. Merck A. G.) and Nb_2O_5 of 99% purity from Fluka A. G. The specimens were sintered at 1050°C for about 100 h to form single-phase solid solutions.

X-ray diffraction powder patterns were taken with a Siemens goniometer at room temperature. The line focus of the Cu tube operating at 35 kV and 20 mA served as the X-ray source. The beam was monochromated by a graphite crystal. The diffracted X-rays were detected with a NaI(Tl) scintillation counter. Each Bragg peak was step-scanned in increments of 0·05°

in 2θ. The resolution of the lines into identifiable components indicated that the specimens were of single phase.

The lattice parameters were determined from the $N=16$ {400} and $N=12$ {222} line groups. The values of the pseudocubic subcell parameters $a_p \sin\beta$, $c_p \sin\beta$ and b_p were obtained directly from the {400} lines. By comparing the half widths of the {400} reflexions (Fig. 1) it can be seen that the first peak actually consists of two components, indicating that c_p is not quite equal to a_p. These peaks were separated by the grid method (Paatero, 1969) with the 040 peak as the 'apparatus' function. The corresponding lattice parameters and those obtained from the neutron diffraction measurements are given in Table 1. β was calculated from the the diffraction lines of the $N=12$ group according to

$$\cos\beta = -\frac{a_p c_p \sin^2\beta}{16}\left[d_{22\bar{2}}^{-2} - d_{222}^{-2}\right].$$

To get reliable intensities from an X-ray diffraction measurement a very careful preparation of the sample is needed to reduce preferred orientation, porosity and surface roughness. Also the separation of the overlapping Bragg peaks is tedious if not impossible in an X-ray pattern. Therefore the X-ray spectra were used only for qualitative considerations.

Neutron diffraction measurements were made at room temperature on a powder diffractometer (D1A) at the high-flux reactor of the ILL, Grenoble. The 20 g powder samples were packed in thin-walled vanadium cans. The wavelength 1·5090 Å from a Ge monochromator was used. The diffractometer was programmed to make steps of 0·05° in 2θ, the counting time being half a minute. The 2θ range from 10° to 140° was covered in about 24 h. Unfortunately, the counting statistics was not as good as expected and therefore the specimens were measured twice and the counts added. The resolution was good and the diffraction pattern quite precise. The observed and calculated profile of the 2 mole % sample is shown in Fig. 2. The background under the peaks was determined by linear interpolation from the regions to which no reflexions contribute. No corrections for absorption or extinction were necessary.

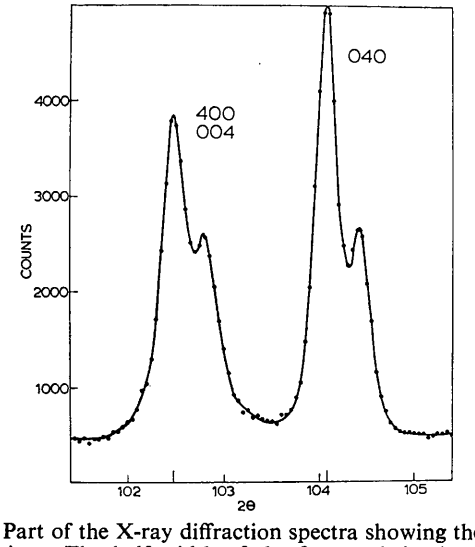

Fig. 1. Part of the X-ray diffraction spectra showing the {400} reflexions. The half width of the first peak is about twice that of the second.

3. Starting models and the profile refinement

The structure was obtained by the procedure described by Hewat (1974*b*).

According to Wells & Megaw (1961) the structure of phase Q is orthorhombic, space group $P2_1ma$ (No. 26, in the *cab* setting). The relation of the unit cell to that of the cubic perovskite is

$$\begin{pmatrix} 1 & 0 & \bar{1} \\ 0 & 2 & 0 \\ 1 & 0 & 1 \end{pmatrix}.$$

[001] and [100] are the face diagonals of the original cube and [010] is parallel to a cube edge. The space group gives the tilt system of the oxygen octahedra as $a^-b^+a^-$.* We checked the tilt system independently from the X-ray spectra. This is possible because the two types of tilts, in phase (+) and antiphase (−), give

* For the notation see Glazer (1972).

Table 1. *The lattice parameters* (Å) *of the* 2 *mole* % *and* 10 *mole* % *samples from X-ray and neutron diffraction measurements*

Sample	X-ray diffraction Pseudocubic	Neutron diffraction* Pseudocubic	Neutron diffraction* Orthorhombic
2 mole % K	a_p= 7·857 (4)	a_p= 7·8567 (6)	a_o=5·5807 (3)
	b_p= 7·767 (2)	b_p= 7·7670 (3)	b_o=7·7670 (3)
	c_p= 7·846 (4)	c_p= 7·8478 (6)	c_o=5·5239 (3)
	β =90·57 (6)°	β =90·586 (3)°	
10 mole % K	a_p= 7·872 (4)	a_p= 7·8782 (7)	a_o=5·5873 (6)
	b_p= 7·792 (2)	b_p= 7·7920 (3)	b_o=7·7920 (7)
	c_p= 7·865 (4)	c_p= 7·8632 (7)	c_o=5·5402 (6)
	β =90·41 (6)°	β =90·479 (4)°	

* Standard errors in brackets do not include error in the neutron wavelength.

rise to independent X-ray reflexions; b^+ produces reflexions such as $\frac{1}{2}0\frac{3}{2}$, $\frac{1}{2}1\frac{3}{2}$ and a^- reflexions such as $\frac{1}{2}\frac{1}{2}\frac{3}{2}$.

The lattice parameters calculated from the {400} lines indicated that the pseudocubic a_p and c_p axes were not equal; this means that the tilt system is in fact $a^-b^+c^-$. Therefore we refined the structure starting from the monoclinic *Pm* (No. 6, in the second setting) (Fig. 3).

Table 2. *Displacements u, v, w from the cubic perovskite positions giving the space group Pm*

		u	v	w
Na, K(1)	1(*a*)	$\frac{1}{4}+u_{Na,K(1)}$	0	$\frac{1}{4}+w_{Na,K(1)}$
Na, K(2)	1(*a*)	$\frac{1}{4}+u_{Na,K(2)}$	0	$\frac{3}{4}+w_{Na,K(2)}$
Na, K(3)	1(*a*)	$\frac{1}{4}+u_{Na,K(3)}$	$\frac{1}{2}$	$\frac{1}{4}+w_{Na,K(3)}$
Na, K(4)	1(*a*)	$\frac{1}{4}+u_{Na,K(4)}$	$\frac{1}{2}$	$\frac{3}{4}+w_{Na,K(4)}$
Nb(1)	2(*c*)	$u_{Nb(1)}$	$\frac{1}{4}+v_{Nb(1)}$	$w_{Nb(1)}$
Nb(2)	2(*c*)	$u_{Nb(2)}$	$\frac{1}{4}+v_{Nb(2)}$	$\frac{1}{2}+w_{Nb(2)}$
O(1)	1(*a*)	$u_{O(1)}$	0	$w_{O(1)}$
O(2)	1(*a*)	$u_{O(2)}$	0	$\frac{1}{2}+w_{O(2)}$
O(3)	1(*b*)	$u_{O(3)}$	$\frac{1}{2}$	$w_{O(3)}$
O(4)	1(*b*)	$u_{O(4)}$	$\frac{1}{2}$	$\frac{1}{2}+w_{O(4)}$
O(5)	2(*c*)	$u_{O(5)}$	$\frac{1}{4}+v_{O(5)}$	$\frac{1}{4}$
O(6)	2(*c*)	$\frac{1}{4}$	$\frac{1}{4}+v_{O(6)}$	$w_{O(6)}$
O(7)	2(*c*)	$u_{O(7)}$	$\frac{1}{4}+v_{O(7)}$	$\frac{3}{4}$
O(8)	2(*c*)	$\frac{1}{4}$	$\frac{1}{4}+v_{O(8)}$	$\frac{1}{2}+w_{O(8)}$

In Table 2 the atomic coordinates are written in terms of the displacements u, v and w from the special positions of the ideal perovskite structure. Assuming that the undistorted octahedra are tilting as rigid units we get for the displacements of the oxygen atoms:
tilt around x–a^-

$$-v_{O(5)}=v_{O(7)}=-w_{O(1)}=w_{O(2)}=w_{O(3)}=-w_{O(4)};$$

tilt around y–b^+

$$u_{O(5)}=-u_{O(7)}=-w_{O(6)}=w_{O(8)};$$

tilt around z–c^-

$$-u_{O(1)}=u_{O(2)}=u_{O(3)}=-u_{O(4)}=-v_{O(6)}=v_{O(8)}\,.$$

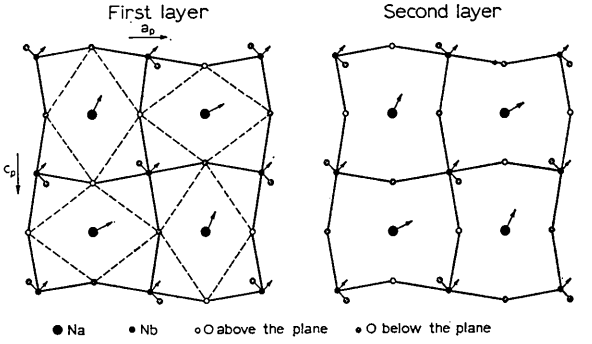

Fig. 3. Plan of the monoclinic structure showing the tilts of the oxygen octahedra ($a^-b^+c^-$). The directions of the Na/K and Nb displacements are indicated by arrows.

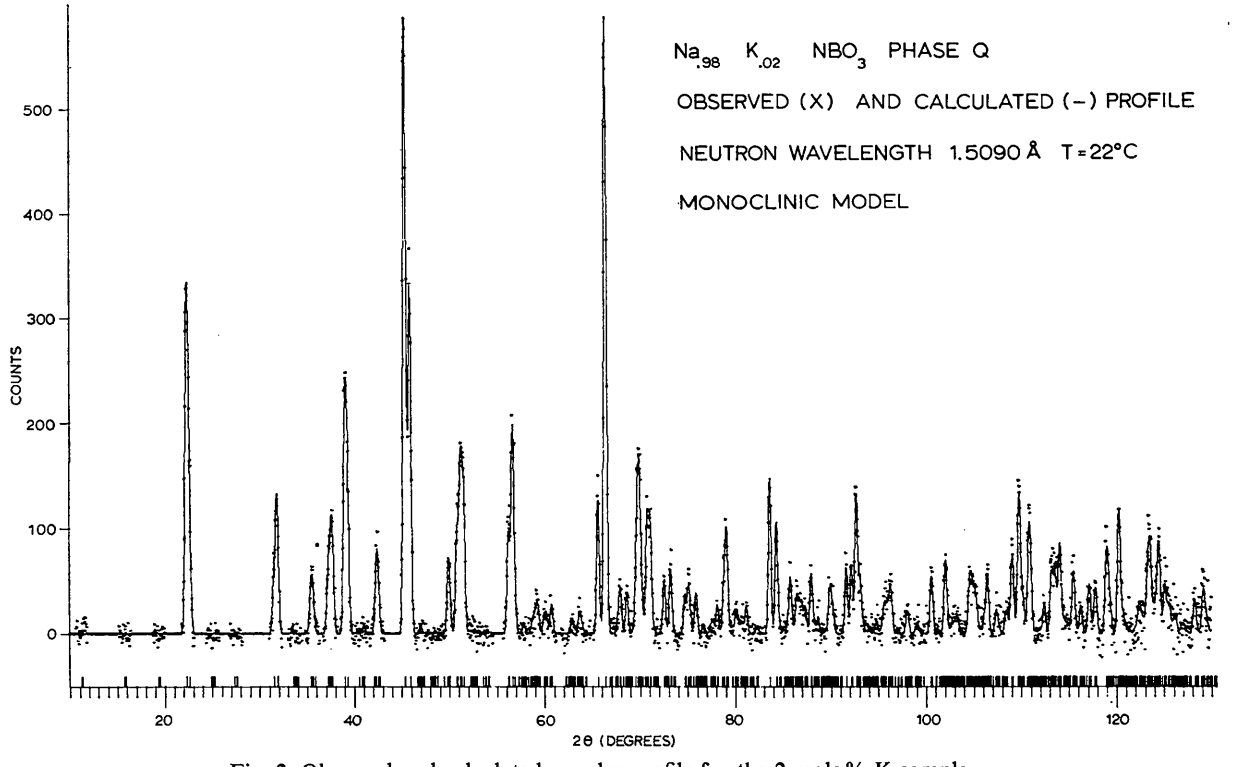

Fig. 2. Observed and calculated powder profile for the 2 mole% K sample.

The Nb atoms were constrained according to the two-corner displacements equal in the two layers, *i. e.*

$$u_{\mathrm{Nb}(1)} = u_{\mathrm{Nb}(2)} = w_{\mathrm{Nb}(1)} = w_{\mathrm{Nb}(2)} ,$$

and the Na, K atoms according to the two different environments caused by the tilting of the octahedra sketched with broken lines in Fig. 3. In addition to the coordinates we refined the scale factor, lattice parameters and temperature factors.

In order to get more meaningful amplitudes we restricted B_{ij} of the oxygen atoms according to the possible vibrations of the rigid octahedra (Fig. 4) as follows:

$$B_{11}(01) = B_{11}(03) = B_{22}(06) = B_{22}(08);$$
$$B_{11}(05) = B_{11}(07) = B_{33}(06) = B_{33}(08);$$
$$B_{22}(05) = B_{22}(07) = B_{33}(01) = B_{33}(03);$$
$$B_{ii}(01) = B_{ii}(02);\ B_{ii}(03) = B_{ii}(04) .$$

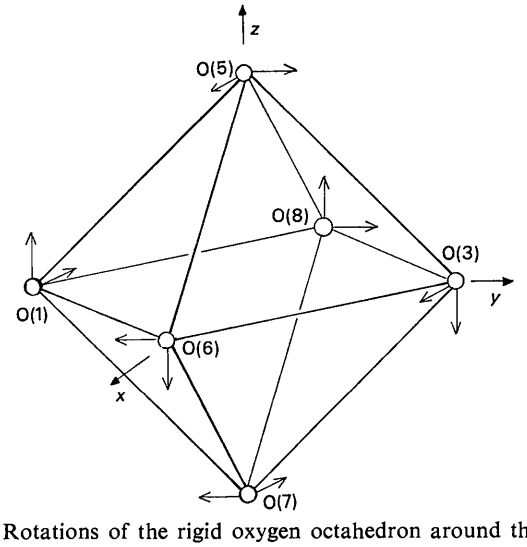

Fig. 4. Rotations of the rigid oxygen octahedron around the axes.

These constraints had only a small effect on the displacement parameters. When the position parameters were constrained their standard deviations fell very low. We could not decide from the data whether or not the oxygen octahedra were slightly distorted, and so to reduce the number of parameters we assumed they were not. The goodness of the fit so obtained justifies this assumption.

In Table 3 the refined displacement parameters are given with the anisotropic temperature factors for both samples. R is defined by

$$R\% = 100 \sum |I_{\mathrm{obs}} - I_{\mathrm{calc}}| / \sum I_{\mathrm{obs}} .$$

They were close to the minimum expected from the statistics.

We also refined the structure as orthorhombic in $P2_1ma$. The fits were nearly as good as with the monoclinic model. No other apparent differences except the splitting of the monoclinic a_p and c_p axes could be detected. This means that the structure of phase Q can be described as very nearly orthorhombic.

Table 4. *Comparison of the interatomic distances* (Å) *in phase Q and in* $KNbO_3$ (*Katz & Megaw*, 1967)

Figures in square brackets give the number of bonds.

	Phase Q		
	2 mole% K	10 mole% K	$KNbO_3$
Nb displacement	0·18	0·19	0·17
Na, K displacement	0·22	0·23	0
Tilt angles			
$\alpha = \gamma$	6·8°	5·2°	0
β	7·8°	7·3°	0
Bond lengths			
Nb–O	1·871	1·874	1·863 [2]
	1·980	1·974	1·991 [2]
	2·127	2·112	2·180 [2]
A–O	2·529	2·568	2·792 [4]
	2·675	2·672	2·854 [4]
	3·161	3·124	2·873 [4]

Table 3. *Atomic parameters of the* 2 *mole* % *and* 10 *mole* % *samples from the monoclinic model*

B_{ij} for a particular atom is defined by the formula for the scattering b_0 corrected by the Debye–Waller factor $b = b_0 \exp\{-[h^2\beta_{11} + k^2\beta_{22} + l^2\beta_{33} + 2hk\beta_{12} + 2hl\beta_{13} + 2kl\beta_{23}]\}$ where $\beta_{ij} = \frac{1}{4}a_i^* a_j^* B_{ij}$.

	2 mole %			10 mole %		
	x	y	z	x	y	z
Na, K(1)	0·264 (2)	0	0·225 (2)	0·268 (2)	0	0·226 (2)
Na, K(2)	0·275 (2)	0	0·736 (2)	0·274 (2)	0	0·732 (2)
Nb(1)	0·0166 (5)	0·251 (2)	−0·0166 (5)	0·0172 (4)	0·250 (1)	−0·0172 (4)
O(1)	−0·029 (2)	0	−0·029 (2)	−0·023 (1)	0	−0·024 (1)
O(5)	0·0342 (4)	0·221 (2)	0·25	0·0321 (4)	0·227 (1)	0·25
O(6)	0·25	0·221 (2)	−0·0342 (4)	0·25	0·226 (1)	−0·0321 (4)
	B_{11}	B_{22}	B_{33}	B_{11}	B_{22}	B_{33}
Na, K(1,2)	1·5 (2)	1·6 (3)	1·5 (2)	1·9 (2)	1·0 (2)	1·9 (2)
Nb(1,2)	0·6 (1)	0·8 (1)	0·6 (1)	0·7 (1)	1·0 (1)	0·7 (1)
O(1–4)	1·6 (6)	0·2 (2)	1·4 (6)	1·2 (3)	0·4 (1)	2·4 (4)
O(5,7)	1·4 (2)	1·4 (6)	0·5 (1)	1·8 (1)	2·4 (4)	0·5 (1)
O(6,8)	0·5 (1)	1·4 (6)	1·4 (2)	0·5 (1)	1·1 (3)	1·7 (1)
		$R = 12{\cdot}0\,\%$			$R = 9{\cdot}2\,\%$	

4. Discussion of the structure

The structure of phase Q belongs to the perovskite family consisting of NbO_3 octahedra connected by shared corners with Na, K statistically distributed in the spaces. Some interatomic distances are collected in Table 4 with the corresponding values of $KNbO_3$.

In the oxygen octahedra the Nb atoms are all displaced in the same direction towards the midpoint of the edge of the surrounding octahedron. This displacement, 0·18 (1) Å in the 2 mole % structure and 0·19 (1) Å in the 10 mole % structure, is about the same as in $KNbO_3$ (0·17 Å). The directions of the Na, K displacements are slightly varied by the O surroundings so that they are displaced along a_p and c_p by 0·12 (2) and 0·20 (2) Å in turn in the 2 mole % structure (Fig. 3).

The octahedra themselves appear to be regular. The regularity of the edges and angles, calculated from the atomic parameters obtained without constraints, justified the use of the constraints. The angles of the octahedral tilts around a_p and c_p were found to be equal in both samples. Across phase Q the tilts decrease with increase of K content from $\alpha=\gamma=6{\cdot}8$ (1)° around a_p and c_p and $\beta=7{\cdot}8$ (1)° around b_p with 2 mole % K to 5·2 (1)° and 7·3 (1)° respectively with 10 mole % K. This decrease is understandable because the larger K atoms then have more space. The same effect is also shown by the different phases of pure $NaNbO_3$ with increasing temperature. In $KNbO_3$ the K atoms have used all the possible space and there are no longer tilts or displacement of K.

The high anisotropy of the temperature factors suggests the presence of a low-frequency zone boundary vibrational mode R_{25} at $\mathbf{q}=(\frac{1}{2}\frac{1}{2}\frac{1}{2})$ corresponding to rotation of the rigid O octahedra round x and z and M_3 at $\mathbf{q}=(\frac{1}{2}\frac{1}{2}0)$ corresponding to rotation around y in accordance with the calculations of Cochran & Zia (1968). Furthermore, in the 10 mole % structure the exceptionally high values of B_{33}[O(1–4)] and B_{22}[O(5,7)] suggest a simple physical explanation for the splitting of a_p and c_p in phase Q.

One of us (MA) acknowledges an exchange grant between France and Finland through the National Research Council for Sciences, Finland, which made the visit to the ILL, Grenoble possible. She is also grateful for having had the opportunity to use the facilities in the ILL and the support of the technical and computing staff there.

References

AHTEE, M. & GLAZER, A. M. (1974). *Ferroelectrics*, **7**, 93–95.
AHTEE, M. & GLAZER, A. M. (1975). To be published.
COCHRAN, W. & ZIA, A. (1968). *Phys. Stat. Sol.* **25**, 273–283.
CROSS, L. E. (1958). *Nature, Lond.* **181**, 178–179.
GLAZER, A. M. (1972). *Acta Cryst.* B**28**, 3384–3392.
HEWAT, A. W. (1973). *J. Phys. C*, **6**, 2559–2572.
HEWAT, A. W. (1974*a*). *Ferroelectrics*, **7**, 83–85.
HEWAT, A. W. (1974*b*). ILL Report.
KATZ, L. & MEGAW, H. D. (1967). *Acta Cryst.* **22**, 639–648.
LEFKOWITZ, I., ŁUKASZEWICZ, K. & MEGAW, H. D. (1966). *Acta Cryst.* **20**, 670–683.
PAATERO, P. (1969). *Ann. Acad. Sci. Fenn.* **VI**, No. 319, 1–58.
RIETVELD, H. M. (1969). *J. Appl. Cryst.* **2**, 65–71.
SAKOWSKI-COWLEY, A. C., ŁUKASZEWICZ, K. & MEGAW, H. D. (1969). *Acta Cryst.* B**25**, 851–865.
TENNERY, V. J. & HANG, K. W. (1968). *J. Appl. Phys.* **39**, 4749–4753.
WELLS, M. & MEGAW, H. D. (1961). *Proc. Phys. Soc.* **78**, 1258–1259.
WOOD, E. A., MILLER, R. C. & REMEIKA, J. P. (1962). *Acta Cryst.* **15**, 1273–1279.